Holographic head-mounted display with RGB light emitting diode light source

Eunkyong Moon,[1] Myeongjae Kim,[2] Jinyoung Roh,[1] Hwi Kim,[1,3] and Joonku Hahn[2,*]

[1]*Department of Electronics and Information Engineering, College of Science and Technology, Korea University, Sejong Campus, South Korea*

[2]*School of Electronics Engineering, Kyungpook National University, Buk-Gu Sankyuk-Dong, Daegu, South Korea*

[3]*hwikim@korea.ac.kr*

[*]*jhahn@knu.ac.kr*

Abstract: A compact head-mounted holographic three-dimensional display with an RGB light-emitting diode (LED) light source is developed. Issues regarding full-color holographic image design and the quality associated with the use of an LED light source are investigated. The accommodation effect and background noise in the proposed system are discussed based on experimental observation.

OCIS codes: (090.1705) Color holography; (090.1995) Digital holography; (120.4825) Optical time domain reflectometry; (090.2820) Heads-up displays.

References and links

1. J. Hong, Y. Kim, H.-J. Choi, J. Hahn, J.-H. Park, H. Kim, S.-W. Min, N. Chen, and B. Lee, "Three-dimensional display technologies of recent interest: principles, status, and issues [Invited]," Appl. Opt. **50**(34), H87–H115 (2011).
2. N. Leister, G. Fütterer, R. Häussler, S. Reichelt, H. Sahm, A. Schwerdtner, A. Schwerdtner, and H. Stolle, "Holographic 3D displays from SeeReal: Developments, improvements, progress," IMID 2009 Digest **2**, 1179–1182 (2009).
3. N. Leister, A. Schwerdtner, G. Fütterer, S. Buschbeck, J.-C. Olaya, and S. Flon, "Full-color interactive holographic projection system for large 3D scene reconstruction," Proc. SPIE **6911**, 69110V (2008).
4. T. Ando, K. Yamasaki, M. Okamoto, and E. Shimizu, "Head-mounted display using a holographic optical element," Proc. SPIE **3293**, 183–189 (1998).
5. O. Cakmakci and J. Rolland, "Head-worn displays: A review," J. Disp. Technol. **2**(3), 199–216 (2006).
6. T. Ando, T. Matsumoto, H. Takahashi, and E. Shimizu, "Head mounted display for mixed reality using holographic optical elements," Mem. Fac. Eng. **40**, 1–6 (1999).
7. H.-E. Kim, N. Kim, H. Song, H.-S. Lee, and J.-H. Park, "Three-dimensional holographic display sing active shutter for head mounted display application," Proc. SPIE **7863**, 78631Y (2011).
8. F. Yaraş, H. Kang, and L. Onural, "Real-time phase-only color holographic video display system using LED illumination," Appl. Opt. **48**(34), H48–H53 (2009).
9. K. Sato, A. Sugita, M. Morimoto, and K. Fujii, "Reconstruction of color images at high quality by a holographic display," Proc. SPIE **6136**, 61360V (2006).
10. J. Hahn and H. Kim, "Digital holographic display for a single user," Proc. SPIE **8556**, 85560I (2012).

1. Introduction

In the field of three-dimensional (3D) displays, accommodation-vergence matching has been considered a key factor in realizing truly natural 3D perception. The opposing concept, accommodation-vergence conflict causes the visual fatigue that people suffer from when watching conventional stereoscopic or multi-view 3D displays [1]. Holographic 3D displays, on the other hand, produce natural 3D images with accommodation-vergence matching and 3D cues such as binocular disparity and motion parallax.

In practice, due to the severe limitations in resolution and bandwidth of commercially available spatial light modulators (SLMs), researchers have developed binocular holographic 3D displays with two narrow viewing-window (VW) assigned to the left and right eyes of an observer. Recent exemplary development was reported by the SeeReal [2,3]. With separate VWs, a system with a large display view can be constructed with low-resolution SLM.

Two VWs corresponding to the left and right eyes are created in free space, through which the observer sees holographic 3D images in a stereoscopic fashion. The stereoscopic display function of the system allows the observer to see the vergence cue by combining the optical beam lines delivering the left and right holographic images with binocular disparity and the holographic characteristics creating the accommodation effect for each optical beam lines. One downside is that a holographic display with its narrow VWs requires the observer to stay in a fixed position. To allow the observer to move comfortably, high performance dual eye-tracking system should be equipped with a directional backlight module, which controls the position of the VWs so that the VWs follow tightly the position of the eye pupils.

Head-mounted displays (HMDs), which enable observers to see immersive scenes, have been also been the subject of intense interest, and some have been commercialized for use in various applications [4]. In particular, HMDs are considered promising candidates for 3D displays, though to our knowledge, the development of a head-mounted full color holographic 3D display with an LED light source has yet to be reported. Previous research showed the use of holographic optical elements (HOEs) for replacement of the beam splitters in HMDs [5,6]. A binocular holographic display with active shutters and a monochromatic laser has been designed [7], but the system was not implemented as the head-mountable form because it was constructed on an optical table and quite bulky.

In this paper, we present the design of the compact holographic HMD that can be worn comfortably and provides see-through scene for application in augmented reality. We describe the prototype development, evaluate display performance, and address issues about full-color holographic image design. The accommodation effect and background noise are also discussed based on experimental observation.

The design and analysis of the proposed system are described in Section 2. In Section 3, the implementation and experimental results are presented, followed by the conclusion in Section 4.

2. System design and analysis

In Fig. 1, the conceptual geometry and Zemax design of the proposed holographic HMD are presented. In the prototype, a field-sequential technique is employed with a high speed liquid crystal on silicon (LCoS) SLM synchronized with fast modulation RGB LED light source [8] for generating full-color holographic 3D images [9]. In order to produce a more compact design, the LED light is coupled to a flexible multi-mode fiber and delivered to the inside of the display module. The system is divided into three parts: (i) an RGB LED light source and optical power delivery optics, (ii) an SLM and Fourier filter, and (iii) an eye-piece lens.

A set of RGB LEDs with dominant wavelengths of $625nm$, $528nm$,and $462nm$ was chosen as the light source, extracted from a commercial projector (AAXA M2 micro-projector). The control box embedded in the projector is used for the field-sequential full-color operation synchronizing the LED light source and the LCoS devices. The spectral bandwidths of the RGB LEDs are $18nm$, $38nm$, and $25nm$, respectively. In order to achieve wearability, the light sources are coupled to a multi-mode optical fiber wit core diameter of $200\mu m$ and numerical aperture of 0.39 and delivered to the display module. The core diameter is a control factor for the degree of coherence of LED light. The smaller diameter multimode fiber generates a higher degree of coherent light, which would be better in realizing the holographic inference effect; however the coupling power is extremely limited, reducing system efficiency. In addition, the degree of coherence is a significant factor in controlling expressible depth and the amount of optical speckles, and influencing the accommodation effect. These issues will be discussed later.

A reflection-type LCoS device is used as an SLM that will display off-axis amplitude computer generated holograms (CGHs). In the off-axis amplitude hologram encoding, a complex number, $Ae^{j\theta}$, is represented by the mth macro-pixel composed of two adjacent pixels on the display panel with a pixel pitch of Δx . The first and second pixels are assigned the amplitude signals, $2A\left(\cos\left(k_c\Delta x\left(1/2+m\right)+\theta\right)+1\right)$ and $2A\left(\cos\left(k_c\Delta x\left(-1/2+m\right)+\theta\right)+1\right)$, respectively. Theoretically, the optical field modulated by a macro pixel of width $2\Delta x$ is

#203220 - $15.00 USD Received 16 Dec 2013; revised 28 Feb 2014; accepted 2 Mar 2014; published 13 Mar 2014

optically Fourier-transformed into the optical Fourier domain, where the optical field distribution is separated into the signal term, conjugate term, and DC term as represented in Fig. 2. This is because the desired complex modulated light field, $Ae^{j\theta}$, propagates along the direction of the carrier wave $e^{jk_c x}$, where the carrier wave number is usually set to $k_c = \pi / (2\Delta x)$.

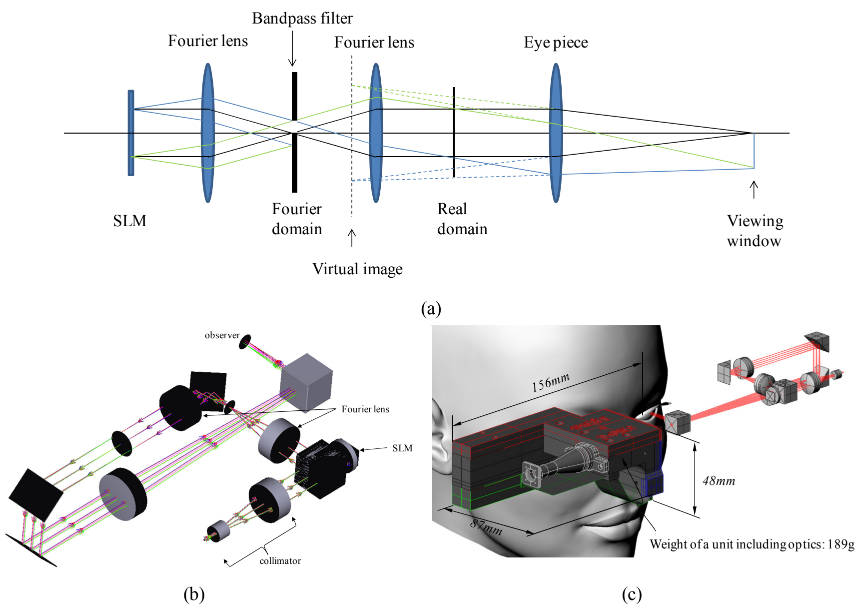

Fig. 1. (a) Concept of optics, (b) Zemax layout of the proposed head-mounted holographic 3D display, and (c) the schematic of the system mounted on observer's head

In the reconstruction process of the complex light field, both the DC and conjugate areas are rejected by the appropriate spatial bandpass filter in the optical Fourier domain; the signal field passed through this filter is to produce complex light field, $Ae^{j\theta}$ at the output plane after the Fourier transform. All pixels of the SLM generate an optical wave bundle with effective complex modulation in the optical Fourier domain cooperatively. As a result, the output signal processed through the $4f$ optics is a complex hologram with the same size as that of the effective area of the SLM and the effective resolution of the display becomes less than half of that of the original panel. The DC noise area can be extended considerably in practice and the signal region passed through the filter is smaller than the half of the total Fourier filtering domain. The extension of the DC region tends to increase as the degree of coherence reduces. In the case of an LED light source, the DC area is extended significantly, which leads to background noise in the holographic images.

The maximum diffraction angle of the SLM is given by

$$\theta = \sin^{-1}(\lambda_B / 2\Delta x) \tag{1}$$

where λ_B is the wavelength of the blue LED and Δx represents the pixel pitch of the SLM. The effective dimension of the Fourier filter plane is given by $\lambda_B f / \Delta x$, which tends to increase along with the wavelength. The filter should treat the R/G/B light fields simultaneously, thus the aperture of the bandpass filter should be located in the intersection region of the signal components in the diffraction patterns of the R/G/B light fields. The maximum intersection area is determined by the blue wavelength. The central wavelength of the blue LED is $462nm$ and the pixel pitch of the SLM is $9.2\mu m$; the maximum diffraction

#203220 - $15.00 USD Received 16 Dec 2013; revised 28 Feb 2014; accepted 2 Mar 2014; published 13 Mar 2014

angle is 1.44deg for this wavelength. The size of the filter is set to reject near half bandwidth area including the conjugate component and DC noise in the optical Fourier domain. For a Fourier lens of focal length $25mm$, the desirable filter size is $0.63mm \times 1.26mm$. After filtering, the amplitude-modulated light field on the SLM plane is transformed into a complex light field representing the CGH.

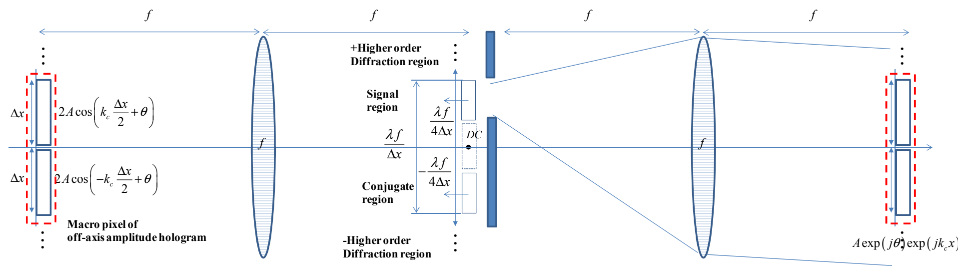

Fig. 2. Off-axis amplitude hologram encoding of $Ae^{j\theta}$ and complex hologram reconstruction with Fourier bandpass filter in 4*f* optical system. The width of the Fourier transformed optical signal is set to $\lambda f / \Delta x$. The centers of the signal field and the conjugate field are located at $x = \lambda f / (4\Delta x)$ and $x = -\lambda f / (4\Delta x)$, respectively, when $k_c = \pi / (2\Delta x)$.

Spatial coherence length is an important factor in determining the view volume expressible by a holographic 3D display [10]. The expressible depth is defined as the depth range where the holographic display can reconstruct spots smaller than the minimum spot size that normal human's eye can resolve correctly. The minimum spot size reconstructed by a hologram is equal to the diffraction-limited spot size in conventional optics. This is based on the assumption that the light source is spatially coherent. However, the spatial coherence length of a light source is finite and in some cases this length is comparable to the aperture size of the optical system. Our concern is to specify the change in the diffraction-limited spot size due to a finite spatial coherence length, which leads to an analysis of the expressible depth of the holographic display. The holographic display reconstructs a cloud of spots in space and these spots are perceived by the eye of the observer. Since the resolvable angle of the human eye is limited, the minimum resolvable spot size is dependent on the distance from the eye. This means the expressible depth of the hologram is not symmetrical with respect to the hologram plane. For example, two spots-one positioned between the hologram plane and the eye, and the other the same distance behind the hologram plane-will be perceived to have the same size. However, the resolvable spot size differs dependent on the distance from the eye. The former is larger than the minimum spot size according to the resolution of the eye, but the latter can be smaller than it.

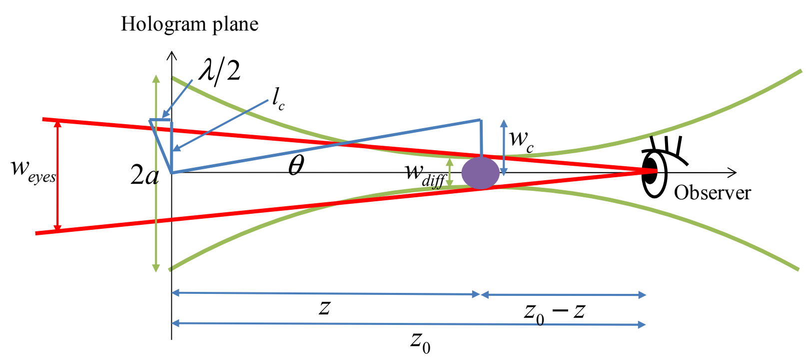

Fig. 3. Increase in the diffraction-limited spot size due to a finite spatial coherence length.

#203220 - $15.00 USD Received 16 Dec 2013; revised 28 Feb 2014; accepted 2 Mar 2014; published 13 Mar 2014

In Fig. 3, the green line indicates the envelope of the optical field that focused at the distance z from the hologram plane. In this case, the spot size is determined by the width of the hologram $2a$. This is the diffraction-limited spot size in conventional optics, given as

$$W_{diff} = 2.44\lambda F/\#, \tag{2}$$

where the F-number is the division of the distance, z by the width of the hologram, $2a$. The limitation of the spatial coherence length leads inevitably to a deviation of the position of the diffraction-limited spot. This deviation is computed from the simple definition of the spatial coherence length on the hologram plane,

$$W_c = \frac{\lambda}{2l_c}|z|. \tag{3}$$

If the distribution of the deviation due to the spatial coherence length is simply assumed to be even, the change in the spot size is a summation of the diffraction-limited spot size and the deviation,

$$W = W_{diff} + W_c = \left(\frac{1.22\lambda}{a} + \frac{\lambda}{2l_c}\right)|z|. \tag{4}$$

When the observer is located at z_0 and watches the spot positioned at z, the minimum resolvable spot size is given by

$$w_{eye} = c(z_0 - z), \tag{5}$$

where c is a constant whose value is 2.91×10^{-4}. This comes from the fact that people usually resolve two spots separated by one minute of arc. It is preferable for the size of the reconstructed spot to be smaller than the resolution of the human eye. Therefore, from Eqs. (4) and (5), the upper and lower bounds for the expressible depth are obtained, respectively, as

$$z < \frac{2caz_0l_c}{a\lambda + 2(ca + 1.22\lambda)l_c} \quad \text{for } z \geq 0, \tag{6a}$$

$$\frac{-2caz_0l_c}{a\lambda - 2(ca - 1.22\lambda)l_c} < z \quad \text{for } z < 0. \tag{6b}$$

Figure 4 shows the change in expressible depth dependent on the spatial coherence length. As previously discussed, for a given spatial coherence length, the expressible depth range is not symmetrical with respect to the origin. Here, the parameters are chosen comparable to those at the experiments described in Section 3 and the coherence length is defined at the image plane of the system. Consequently, the use of an LED source is expected to constrain the expressible depth and increase the background optical noise in the holographic images.

#203220 - $15.00 USD Received 16 Dec 2013; revised 28 Feb 2014; accepted 2 Mar 2014; published 13 Mar 2014

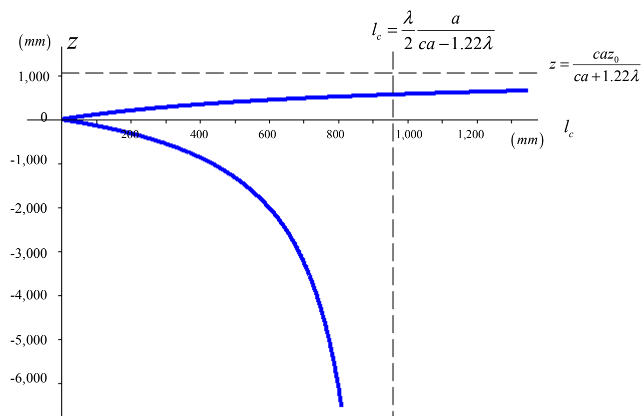

Fig. 4. Change in the expressible depth with respect to spatial coherence length.

The complex holographic field is transferred to the eyepiece that aids the observer to watch magnified holographic images floating in free space. As stated above, the expressible depth range is constraint by the spatial coherence length. When the coherence length approaches to zero, the specified single plane is representable by imaging of the SLM. Let this imaging plane be named by the 'incoherent imaging plane.'

The incoherent imaging plane of the developed prototype is designed to be located $1125mm$ in front of the eye. The sampling interval at the incoherent imaging plane is then given by

$$\Delta x' = \frac{\lambda_B}{2\sin\left[\tan^{-1}\left(h/d\right)\right]}, \tag{7}$$

where d and h are the distance from the eye to the incoherent imaging plane and the short side length of the VW, respectively. We determined that h is set to $3.14mm$, which is compatible with pupil size of the eye. From Eq. (7), the sampling interval, $\Delta x'$ is thus $83\mu m$, nine times the size of the pixel pitch of the SLM. To satisfy these conditions, eyepiece requires a magnification of 9x. The focal length of the eyepiece therefore satisfies the following equations:

$$\frac{1}{f} = \frac{1}{z_S} + \frac{1}{z_I} = -\frac{8}{z_I}, \tag{8a}$$

$$f - z_I = d, \tag{8b}$$

where Eq. (8a) is the imaging equation, and z_S and z_I are the distances from the eyepiece to the SLM and to the incoherent imaging plane, respectively. Since we assume the virtual imaging condition, the sign of the distance z_I is negative. From Eqs. (8a) and (8b), the focal length of the eyepiece is calculated to be $125mm$. In addition, a beam splitter is installed at the VW, in order to enable the observer to watch virtual holographic 3D images and the background real world scene simultaneously as shown in Fig. 1(b); this enables its use in augmented reality applications.

#203220 - $15.00 USD Received 16 Dec 2013; revised 28 Feb 2014; accepted 2 Mar 2014; published 13 Mar 2014

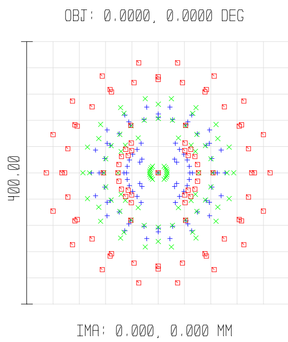

(a)

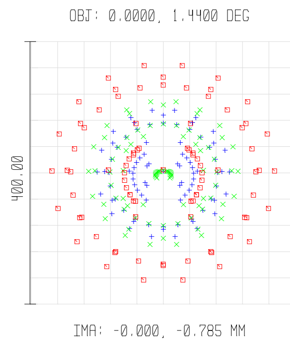

(b)

Fig. 5. Spot diagram at the VW with the incident fields (a) parallel to the optical axis, and (b) at an oblique angle of 1.44deg. Here, the red, green, and blue symbols represent a bundle of rays with the different wavelengths 625nm, 528nm, and 462nm, respectively.

To evaluate the overall optical performance of the designed system, we analyze the spot diagram of our system at the VW in Fig. 5. The spot diagram in Fig. 5(a) presents the collimation quality for the normal incidence of light. Figure 5(b) shows the spot diagram for the oblique incidence of light set at 1.44deg (the maximum diffraction angle of the SLM). Here, the red, green, and blue symbols each represent a bundle of rays with the wavelengths $625nm$, $528nm$, and $462nm$, respectively. In our system, a field with an obliquity of 1.44deg represents the marginal field with the maximum directional cosine without vignetting. Actually, because we use off-the-shelf optic components, the spot radius is not optimized to the theoretical limit. The RMS radiuses of the spots in Figs. 5(a) and 5(b) are measured as $98.0\mu m$ and $95.7\mu m$, respectively. These sizes are very small in comparison to the size of the VW. However, it would be possible to compensate for those aberrations by aberration-compensated hologram encoding technique.

3. Experimental results

The prototype system has been developed with the aid of 3D printer fabrication technology and all optical elements used in the development are off-the-shelf components. Figure 6 shows the proposed head-mounted holographic display module and its control box. The head-mounted holographic display module is compact and wearable with the dimensions of $156mm \times 85mm \times 48mm$. The light sources and control board for the SLM are installed inside the control box. As shown in Fig. 6(b), the control box contains two compartments. In the upper compartment, the control board is attached; the lower contains the LED light sources, the beam-combining optics, and the fiber-coupling optics. The RGB LEDs are packed tightly and their beam lines are collinearly aligned through a beam combiner and shaped by a homogenizer. The light is coupled to an optical fiber with a collimator for an FC/PC connector. The control board receives a video signal from an HDMI connector. The light sources from the three LEDs with different wavelengths are temporally multiplexed by the control board and synchronized to the SLM. The control signals are communicated by a ribbon data cable.

#203220 - $15.00 USD Received 16 Dec 2013; revised 28 Feb 2014; accepted 2 Mar 2014; published 13 Mar 2014

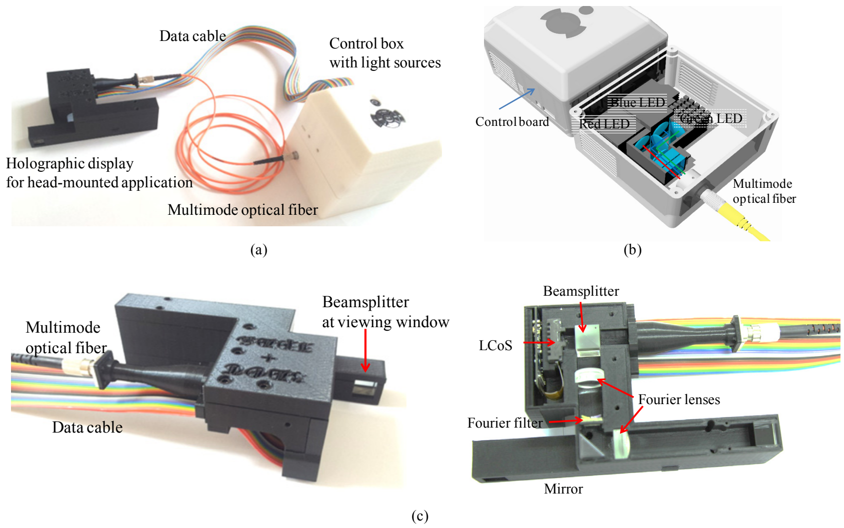

Fig. 6. (a) Full head-mounted holographic display system, (b) control box with RGB LEDs fed to a multimode optical fiber and (c) optics of the holographic display module

For the experimental demonstration, a simple CGHs composed of the letters, ‘A’, and ‘B’ separated by 50cm is calculated for the R/G/B wavelengths. The letter ‘A’ is located on the incoherent imaging plane, and the letter ‘B’ is placed in front of the incoherent imaging plane. In Fig. 7(a), the off-axis amplitude CGH for green light is presented and the numerical simulation results of the observation are shown in Figs. 7(b) and 7(c). The simulation results visualize a clear accommodation effect in the CGH examples. In the experiment, the CGH patterns were prepared for blue and red lights. In Fig. 8, images from the experiment captured with a DSLR camera are presented, One focused on the ‘A’ on the left and the other focused on the ‘B’ on the right. The holographic display can successfully express multiple planes focused at different depths, even with a partially coherent LED light source.

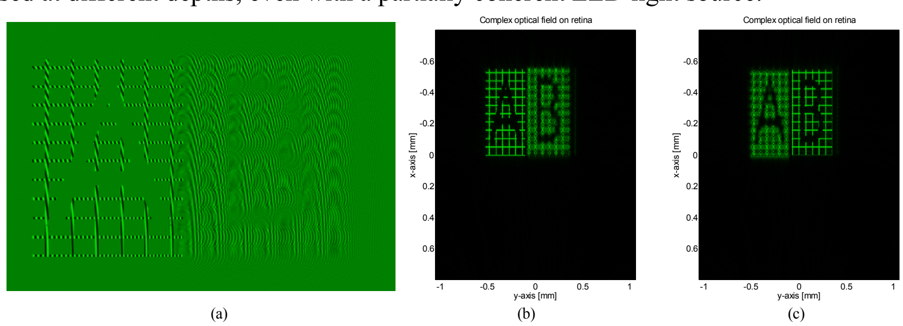

Fig. 7. Simulation result: (a) off-axis amplitude CGH pattern and observation, with a focus on (b) ‘A’ and (c) ‘B’ for a green coherent light field.

Comparing the experimental results with the simulation results, we note that the use of a partially coherent LED light source can produce background noise. The clear expression of black or dark fields is crucial for display, but the non-ideal collimation prevents the complete filtering of the DC component in the Fourier filter plane, which generates bright background noise and reduces the darkness or the contrast ratio. In the experiment, we observed a broader DC spot in the Fourier filter plane. A necessary test is to check the image quality with respect to the fiber core size. The smaller the core size, the tighter the DC spot which can be obtained in the Fourier filter plane; in this case, however, the coupling loss increases weakening the brightness. To resolve this engineering problem, further research into image quality and optical coherence is necessary.

#203220 - $15.00 USD Received 16 Dec 2013; revised 28 Feb 2014; accepted 2 Mar 2014; published 13 Mar 2014

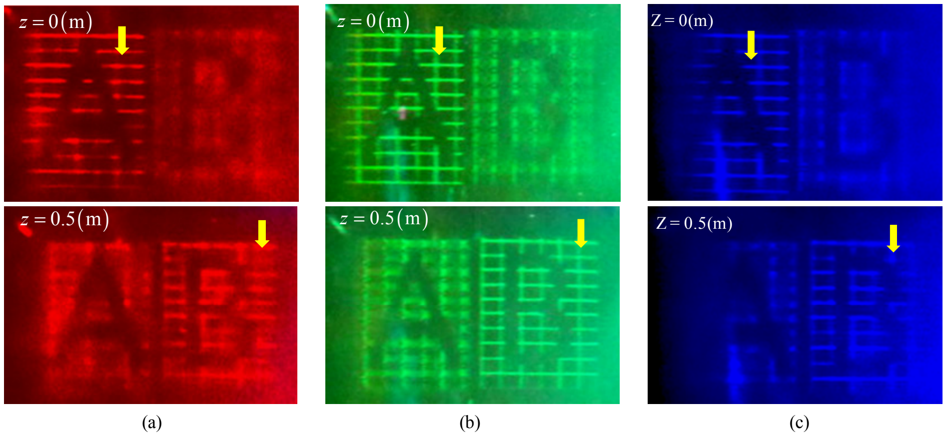

Fig. 8. Captured images with the camera set focused at different distances when (a) red, (b) green, and (c) blue LEDs are turned ON respectively.

From a theoretical point of view, the accommodation effect of a voxel is maximized when the light rays emanating from the voxel have a wide spatial angular frequency or a wide diverging angle in its light field profile. In holographic imaging, speckle indicates an irregularity in the phase distribution of the light field. In this case, the phase relationship between adjacent voxels is not correlated, meaning that the light field from each holographic voxel emits fully divergent light. This leads to the maximum accommodation effect in human perception. A byproduct of phase irregularity is the contamination of the holographic image with speckle. However, in our proposed system, LED light with controlled partial coherence can greatly reduce the speckle pattern by smoothing it. Consequently, it is expected that an LED light source can provide a better accommodation perception cue than a laser source if the degree of coherence of light source is optimized to maximize the accommodation effect and smooth speckles out simultaneously.

5. Conclusion

We have developed a compact, color holographic HMD prototype with an LED light source, and proven the system feasible. With this prototype, we have explored the fundamental aspects behind the use of RGB LED light sources in holographic 3D displays. The influence of the degree of coherence on the expressible depth and the accommodation was also discussed. Optimal tuning of the degree of coherence of LED light sources is crucial in achieving the highest holographic image quality. Also, we have described the prototype of right-side monocular module. Basically, the HMD should be a binocular system composed of two monocular systems. An important thing to be considered for the binocular HMD system is the binocular calibration to match the convergence of left and right eyes. The holographic volume spaces of the left and right parts should create three-dimensionally aligned holographic volume space in the intersection volume of their volume spaces. The other point is that a person has his/her own interpupillary distance. The tuning nob that can control the interpupillary distance is a basic mechanics in commercial stereoscopic HMDs.

Based on this preliminary study, we will continue to explore the subjects for finding the optimal coherence condition of light source for holographic 3D displays and work on the engineering issues associated with binocular system.

Acknowledgments

This research was supported both by Basic Science Research Program through the National Research Foundation of Korea (NRF) funded by the Ministry of Education, Science and Technology (2012R1A1A1014417) and (2010-0022088). Joonku Hahn is the corresponding author and Hwi Kim is the co-corresponding author.